BULLETIN OF THE POLISH ACADEMY OF SCIENCES
TECHNICAL SCIENCES, Vol. 70(1), 2022, Article number: e139003
DOI: 10.24425/bpasts.2021.139003

Preliminary modelling methodology of a coupled payload-vessel system for offshore lifts of light and heavyweight objects

Anna MACKOJC* and **Bogumil CHILINSKI**

Institute of Machine Design Fundamentals, Warsaw University of Technology, Poland

Abstract. This paper presents the concept of the modelling methodology of a payload-vessel system allowing for a comprehensive investigation of mutual interactions of the system dynamics for lifting in the air. The proposed model consists of six degrees of freedom (6-DoF) vessel and three degrees of freedom (3-DoF) lifting model that can replace the industrial practice based on a simplified approach adopted for light lifts. Utilising the response amplitude operators (RAOs) processing methodology provides the ability to incorporate the excitation functions at the vessel crane tip as a kinematic and analyse a wide spectrum of lifted object weights on a basis of regular wave excitation. The analytical model is presented in detail and its solution in a form of numerical simulation results are provided and discussed within the article. The proposed model exposes the disadvantages of the models encountered in engineering practice and literature and proposes a novel approach enabling efficient studies addressing a lack of access to reliable modelling tools in terms of coupled models for offshore lifting operations planning.

Key words: offshore lifting modelling; coupled payload-vessel model; payload pendulation.

1. INTRODUCTION

One of the challenges encountered during offshore operations is naturally a necessity of dealing with the surrounding environment. When considering operations of lifting in the air whilst at sea, the biggest accompanying factor to withstand is a sea state that when being unfavourable might considerably reduce the operating window or increase the risk. In order to assist the industry, several operational practices have been developed but there is still limited access to a proper, simple, dynamic modelling tool coupling the dynamics of both the lifted object and vessel. This raises a need for appropriate understanding of the mutual relationship between the behaviour of the payload and that of the vessel. That would allow the proposal of an effective methodology and lead to a reliable tool that might increase the operational efficiency and safety in terms of dynamic behaviour analysis and operation design and planning.

When discussing any lifting operation undertaken offshore, a distinction between two phases can be made. These include particularly handling the payload in the air and lowering it in water. Many publications addressing the problem of offshore lifting operations can be found, however, in the vast majority they address numerical analyses of heavy lifts concerning coupled models with a particular focus on the lowering process only. This leaves a scientific and industrial gap to consider an equally important part of an offshore lift operation – lifting in the air. This is the phase that carries the greatest risk of resonance vibrations occurrence, and thus the uncontrolled motion of large amplitudes. Moreover, due to a wide range of weights of structures installed, it is essential to study the mutual dynamics between the lifted weight and the lifting vessel and determine the limit of the applicability of simplified models, which are widely proposed within the literature. The importance of setting such a limit is shown in the article [1], where the authors describe the methodology based on a specific case study of an installation of an offshore wind turbine monopile installation. This methodology, however, is not universal as it focuses on a very specific operation. The importance and complexity of offshore operations safety issue are also shown in [2], where the authors discuss and seek a method of control algorithm for a ship dynamic positioning with a neural network in order to reduce dependency on the determination of ship hydrodynamic coefficients.

The study [3] presents a numerical model of the coupled system of a monopile for an offshore wind turbine and a vessel. Numerical simulations are provided paying attention only to the lowering phase of the lifting operation. A similar focus might be found in [4] where the authors address the numerical analysis of the installation of a tripod foundation using a heavy lift vessel. In [5] and [6], the authors studied the dynamic behaviour of an offshore crane cable and its unstable states referred to as a parametric resonance vibration. The analysis was conducted for long cables only, used in subsea lowering operations. In the article [7], the authors present a dynamic model of a floating crane vessel with a hanging load. The model is defined as a linearized coupled double pendulum problem, as the pendulation of the suspended mass was limited by the assumption of small displacements. A similar simplification is presented in [8], where the authors propose a method for double pendulum cranes for minimisation of energy consumption when fulfilling the transportation tasks. Other simple models might

*e-mail: anna.mackojc@pw.edu.pl

Manuscript submitted 2021-04-07, revised 2021-06-24, initially accepted for publication 2021-08-19, published in February 2022.

be found in [9–11], where the lifting model is presented as a single pendulum, where excitation is incorporated as an angular roll, ignoring the heave and the potential influence of the vessel. This methodology eliminates the ability to capture the parametric resonance. In [12], the authors look for approximate analytical solutions for a model of the parametric pendulum. The system was modelled as a mathematical pendulum being excited by means of vertical harmonic force. The approximated solutions were found for oscillations and rotations of the pendulum. Although the model is not discussed in the context of the lifted payload specifically, the presented model is still a better representation as it does not neglect an importance of the vertical excitation. The authors of [13] investigate the dynamics of a parametrically induced spherical pendulum. They consider a moving support analysing the pendulum dynamics based on governing equations derived from the system energy formulation. The presented single degree of freedom model is analysed in the Cartesian coordinates, which may not be intuitive for interpretation purposes of a pendulum motion.

A little bit more complicated model is proposed in [14]. The authors model and study the dynamics of dual cranes carrying a distributed-mass beam and propose the control algorithm by predicting and incorporating the natural frequency of the system. On the other hand, one might encounter an overly complex model proposals, where the study is based on a single, particular case preventing a reliable assessment of the whole phenomena. Such models can be found in [15] and [16]. The authors of [15] propose a pendulation control by an enormous number of lifting wires and hence multiple cranes or complex machinery involved.

The article [17] describes a rapid development in the field of offshore renewable energy, particularly in the wind farms sector, where newly built turbines are to be installed mainly on the Baltic Sea area. That requires a huge effort to be put into the installation process of every single structure. This is related to the effective planning of maritime operations by a development of dynamic models allowing the simulation of behaviour and mutual relation of payload-vessel systems at sea during the installation. Moreover, as there are records reporting heavy lift operations focusing only on a lowering phase, where the payload pendulation is naturally suppressed by the water, the authors decided to propose a modelling methodology of a coupled payload-vessel system allowing for a reliable assessment of the lifted objects-vessel dynamic behaviour when handling in the air. The proposed model enables analyses in a whole spectrum of lifted objects whether these are light or heavyweights.

2. OBJECTIVES AND OVERVIEW

Lifting operations are a relevant part of many offshore activities. In order to complete operations successfully, the operators have to manage environmental phenomena sometimes leading to significant limitations. Critical cases occur in the lifting zone, where the payload-cable system behaves llike a pendulum with a moving pivot point. This might cause the payload to be loaded by external forces, which lead to resonance phenomena. Depending on the type of vibrations, angular vibrations of the payload due to parametric or forced resonance may be observed. These hazardous phenomena raise the necessity for the creation of simple and accessible tools allowing for their prediction.

The dynamics of heavy payloads cannot be considered independently to the vessel movement. DNV (DET NORSKE VERITAS) codes present a simplified approach for light lifts regime, where the mass of the payload is no greater than 2% of the floating unit displacement. For light lifts the crane boom can be treated as a stiff structure, hence the motion of the crane tip can be determined directly from the wave-induced rigid body motion of the vessel. The wave-induced translational motions (surge, sway and heave) of the crane tip are given from the vessel RAOs (response amplitude operators) for six degrees of freedom motion usually defined for the centre of gravity for the vessel [18–21]. The aim of this study is to propose a coupled model, which is sensitive to changes of the system parameters and allows for a comprehensive investigation of the system dynamics during the lifting in the air phase.

The study concerns 6 degrees of freedom related of the vessel, providing the linear and angular motions directly coupling the two considered systems. Floating units might be considered as continuous systems that when operating, are subjected to complex motions, which might be decomposed into a rigid body motion and its vibrations. In practice, the vessel elastic properties are omitted as the naval designs are stiff enough, which allows the adoption of a simple model of a rigid body in analytical considerations. Hence the hydrodynamic forces might be represented as hydrodynamic added mass, fluid damping and restoring forces. The vessel excitation is modelled as one-directional forward propagating waves. The lifting system is composed of a crane tip equipped with a lifting cable with length-dependent stiffness. The 3 degrees of freedom are related to the payload and compensator masses and also their pendulation as referred in [22]. The research outlines a novel approach produced in cooperation between the authors and Fathom Group Ltd.

The usefulness and further application of the proposed model shall be validated. The authors stated that ensuring convergence with the 3-DoF model for light lifts will be crucial from the point of view of the proposed model verification. For this purpose, a comparative analysis was initially proposed of the payload and vessel response for a number of different payload masses. According to the authors, this enables verification of the advantages of the coupled model that might be utilised in both, light and heavyweight objects regimes. Moreover, the proposed approach allows the user to analyse the impact of the vessel and payload properties on the system dynamics.

3. PROPOSED COUPLED MODEL FOR OFFSHORE LIFTS

The behaviour of 9-DoF model being composed of 6-DoF vessel and 3-DoF lifting system model must be considered. The vessel, as mentioned in Section 2, is modelled as a rigid body excited by forces caused by a hydrodynamic interaction with the hull. For the 3-DoF model, the description is similar to the modelling process of an elastic pendulum.

The following equations represent the total energy of the system under consideration presented in Fig. 1. It was possible to determine kinetic and potential energies of the subsystems in the analytical manner based on [22].

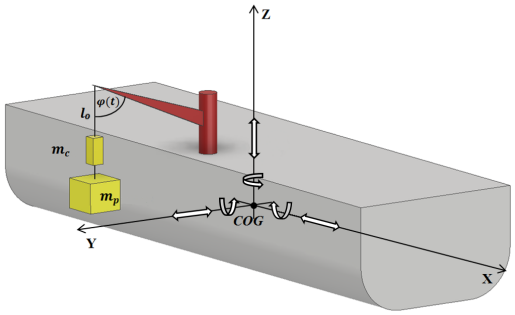

Fig. 1. A 6-DOF vessel with the 3-DOF lifting system and its parameters

The kinetic energy (1) was determined as a sum of the energy of all the system masses (payload and compensator). The T_p formula has the following representation:

$$T_p = \frac{m_c\left(\dot{y}_c^2+\dot{z}_c^2\right)}{2}+\frac{m_p\left(\dot{y}_p^2+\dot{z}_p^2\right)}{2}. \tag{1}$$

The potential energy of the system discussed results from the presence of a homogeneous gravitational field and the two springs representing respectively the cable stiffness k_w and the stiffness of the compensator k_c. The equation describing V_p is given in (2):

$$V_p = -gm_cz_c - gm_pz_p + \frac{k_c\left(-h_{ceq}+h_{eq}+h-h_c\right)^2}{2} + \frac{k_w\left(h_{ceq}+h_c\right)^2}{2}. \tag{2}$$

The kinetic energy T_v related to the vessel structure motion resulting from the wave excitation is provided by the relation presented in (3):

$$T_v = \frac{I_5\left(-\frac{A_h\omega\sin\left(\phi_w\right)\ddot{\phi}_w}{g}-\frac{A_h\omega\cos\left(\phi_w\right)\dot{\phi}_w^2}{g}+\dot{\Phi}\right)^2}{2} + \frac{M_{\text{vessel}}\left(-A_h\sin\left(\phi_w\right)\dot{\phi}_w+\dot{H}\right)^2}{2}. \tag{3}$$

The potential energy of the vessel is expressed based on a hydrostatic stability of the structure and is given as presented in eqrefeq:Vvessel:

$$V_v = \frac{\left(-A_{wl}g\rho\left(-CoB+CoF\right)H+GM_LVg\rho\Phi\right)\Phi}{2} + \frac{\left(-A_{wl}g\rho\left(-CoB+CoF\right)\Phi+A_{wl}g\rho H\right)H}{2}, \tag{4}$$

where:

$(\varphi,\ h,\ h_c)$ – payload generalized coordinates,
t – independent variable (time),
m_p – mass of payload,
k_w – wire stiffness,
l_0 – length of the lifting cable,
l_w –length of the lifting cable-payload system,
$R\sin\left(-\frac{A_h\omega\sin(\phi_w)\dot{\phi}_w}{g}+\alpha+\Phi\right)$ – lateral displacement at crane tip obtained from RAOs (a regular wave excitation),
$A_h\cos(\phi_w)+R\cos\left(-\frac{A_h\omega\sin\left(\phi_w\right)\dot{\phi}_w}{g}+\alpha+\Phi\right)+H$ – vertical displacement at crane tip obtained from RAOs (a regular wave excitation),
m_c – mass of compensator,
k_c – stiffness of heave compensator,
l_c –length of the attached compensating element,
g –acceleration of gravity,
h_{eq} – equilibrium point of payload,
h_{ceq} – equilibrium point of compensator,
M_{vessel} – mass of vessel,
I_5 – moment of inertia of 5-th degree (with respect to y axis, determined by the radius of gyration),
$(H,\ \Phi)$ – vessel generalized coordinates,
$A_h\cos(\phi_w)$ – wave level,
$-\frac{A_h\omega\sin(\phi_w)\dot{\phi}_w}{g}$ – wave slope,
ρ – fluid density,
g – acceleration of gravity,
A_{wl} – wetted area,
V – submerged volume of the vessel,
GM_L – longitudinal metacentric height,
CoB – centre of buoyancy,
CoF – centre of floatation.

In order to obtain governing equations, the methods of Lagrangian mechanics were adopted. Based on the obtained Lagrangian of the entire system, governing equations were found. Hence, the considered payload-vessel system might be modelled by the following matrix equations (5), (6):

$$\left(M_V+A\right)\cdot\ddot{X}(\omega,\text{dir})+C_V\cdot\dot{X}(\omega,\text{dir})+K_V\cdot X(\omega,\text{dir}) = F(\omega,\text{dir}), \tag{5}$$

$$M_P(t)\cdot\ddot{X}+G_P\left(t,\dot{X}\right)\cdot\dot{X}+C_P(t)\cdot\dot{X}+K_P(t)\cdot X = F(\dot{X},X,t), \tag{6}$$

where:

M_V – mass matrix of the vessel,
A – hydrodynamic added mass matrix,
C_V – hydrodynamic damping matrix,
K_V – vessel stiffness matrix,
$F(\omega,\text{dir})$ – hydrodynamic force vector,
ω – natural frequency,
dir – wave direction,
M_P – inertia matrix of payload,
G_P – payload gyroscopic matrix,
C_P – damping matrix of payload,
K_P – payload stiffness matrix.

The fundamental matrix obtained from the system of governing equations might be represented by relations of the system parameters. Their mutual relations and assumptions allowed to introduce some simplifications to the system Lagrangian. The dependencies used are as follows:

$$h_{eq} = l_0 \nu \,, \tag{7}$$

$$h_{ceq} = l_0 \nu \,, \tag{8}$$

$$k_c = \frac{m_p}{10} \,, \tag{9}$$

$$R = l_0 \,, \tag{10}$$

$$l_c = \frac{l_0}{10} \,, \tag{11}$$

$$A_h = \gamma l_0 \,, \tag{12}$$

$$\omega = \frac{\sqrt{g}\mu}{\sqrt{l_0}} \,. \tag{13}$$

$$\phi_w = \Phi_h + \omega t \,, \tag{14}$$

where: ν, μ, γ – simplifying proportionality factors.

A general form of the system fundamental matrix and its particular elements are given as:

$$A = \begin{bmatrix} A_{11} & A_{12} & A_{13} & 0 & A_{15} \\ A_{21} & A_{22} & A_{23} & A_{24} & A_{25} \\ A_{31} & A_{32} & A_{33} & A_{34} & A_{35} \\ 0 & A_{42} & A_{43} & A_{44} & A_{45} \\ A_{51} & A_{52} & A_{53} & A_{54} & A_{55} \end{bmatrix} . \tag{15}$$

Each of the elements of matrix A is presented in details as an individual equation:

$$\begin{aligned} A_{11} = &-\frac{11\Omega^2 l_0^2 m_p \nu^2}{10} - \frac{12\Omega^2 l_0^2 m_p \nu}{5} - \frac{131\Omega^2 l_0^2 m_p}{100} \\ &+ \frac{11 g\gamma^2 l_0 m_p \mu^6 \nu \cos\left(\gamma\mu^2 \sin\left(\phi_w\right)\right)\cos^2\left(\phi_w\right)}{10} \\ &+ \frac{6 g\gamma^2 l_0 m_p \mu^6 \cos\left(\gamma\mu^2 \sin\left(\phi_w\right)\right)\cos^2\left(\phi_w\right)}{5} \\ &- \frac{11 g\gamma l_0 m_p \mu^4 \nu \sin\left(\gamma\mu^2 \sin\left(\phi_w\right)\right)\sin\left(\phi_w\right)}{10} \\ &- \frac{6 g\gamma l_0 m_p \mu^4 \sin\left(\gamma\mu^2 \sin\left(\phi_w\right)\right)\sin\left(\phi_w\right)}{5} \\ &+ \frac{11 g\gamma l_0 m_p \mu^2 \nu \cos\left(\phi_w\right)}{10} + \frac{6 g\gamma l_0 m_p \mu^2 \cos\left(\phi_w\right)}{5} \\ &+ \frac{11 g l_0 m_p \nu}{10} + \frac{6 g l_0 m_p}{5} \,, \end{aligned} \tag{16}$$

$$\begin{aligned} A_{12} = &\, g\gamma^2 m_p \mu^6 \sin\left(\gamma\mu^2 \sin\left(\phi_w\right)\right)\cos^2\left(\phi_w\right) \\ &+ g\gamma m_p \mu^4 \sin\left(\phi_w\right)\cos\left(\gamma\mu^2 \sin\left(\phi_w\right)\right) \,, \end{aligned} \tag{17}$$

$$\begin{aligned} A_{13} = &\, \frac{g\gamma^2 m_p \mu^6 \sin\left(\gamma\mu^2 \sin\left(\phi_w\right)\right)\cos^2\left(\phi_w\right)}{10} \\ &+ \frac{g\gamma m_p \mu^4 \sin\left(\phi_w\right)\cos\left(\gamma\mu^2 \sin\left(\phi_w\right)\right)}{10} \,, \end{aligned} \tag{18}$$

$$\begin{aligned} A_{15} = &-\frac{11\Omega^2 l_0^2 m_p \nu \cos\left(\gamma\mu^2 \sin\left(\phi_w\right)\right)}{10} \\ &- \frac{6\Omega^2 l_0^2 m_p \cos\left(\gamma\mu^2 \sin\left(\phi_w\right)\right)}{5} \\ &- \frac{11 g\gamma^2 l_0 m_p \mu^6 \nu \cos\left(\gamma\mu^2 \sin\left(\phi_w\right)\right)\cos^2\left(\phi_w\right)}{10} \\ &- \frac{6 g\gamma^2 l_0 m_p \mu^6 \cos\left(\gamma\mu^2 \sin\left(\phi_w\right)\right)\cos^2\left(\phi_w\right)}{5} \\ &+ \frac{11 g\gamma l_0 m_p \mu^4 \nu \sin\left(\gamma\mu^2 \sin\left(\phi_w\right)\right)\sin\left(\phi_w\right)}{10} \\ &+ \frac{6 g\gamma l_0 m_p \mu^4 \sin\left(\gamma\mu^2 \sin\left(\phi_w\right)\right)\sin\left(\phi_w\right)}{5} \,, \end{aligned} \tag{19}$$

$$\begin{aligned} A_{21} = &\, g\gamma^2 m_p \mu^6 \sin\left(\gamma\mu^2 \sin\left(\phi_w\right)\right)\cos^2\left(\phi_w\right) \\ &+ g\gamma m_p \mu^4 \sin\left(\phi_w\right)\cos\left(\gamma\mu^2 \sin\left(\phi_w\right)\right) \,, \end{aligned} \tag{20}$$

$$A_{22} = -\Omega^2 m_p + k_c \,, \tag{21}$$

$$A_{23} = -k_c \,, \tag{22}$$

$$A_{24} = -\Omega^2 m_p \,, \tag{23}$$

$$\begin{aligned} A_{25} = &-\Omega^2 l_0 m_p \sin\left(\gamma\mu^2 \sin\left(\phi_w\right)\right) \\ &- g\gamma^2 m_p \mu^6 \sin\left(\gamma\mu^2 \sin\left(\phi_w\right)\right)\cos^2\left(\phi_w\right) \\ &- g\gamma m_p \mu^4 \sin\left(\phi_w\right)\cos\left(\gamma\mu^2 \sin\left(\phi_w\right)\right) \,, \,, \end{aligned} \tag{24}$$

$$\begin{aligned} A_{31} = &\, \frac{g\gamma^2 m_p \mu^6 \sin\left(\gamma\mu^2 \sin\left(\phi_w\right)\right)\cos^2\left(\phi_w\right)}{10} \\ &+ \frac{g\gamma m_p \mu^4 \sin\left(\phi_w\right)\cos\left(\gamma\mu^2 \sin\left(\phi_w\right)\right)}{10} \,, \end{aligned} \tag{25}$$

$$A_{32} = -k_c \,, \tag{26}$$

$$A_{33} = -\frac{\Omega^2 m_p}{10} + k_c + k_w \,, \tag{27}$$

$$A_{34} = -\frac{\Omega^2 m_p}{10} \,, \tag{28}$$

$$\begin{aligned} A_{35} = &-\frac{\Omega^2 l_0 m_p \sin\left(\gamma\mu^2 \sin\left(\phi_w\right)\right)}{10} \\ &- \frac{g\gamma^2 m_p \mu^6 \sin\left(\gamma\mu^2 \sin\left(\phi_w\right)\right)\cos^2\left(\phi_w\right)}{10} \\ &- \frac{g\gamma m_p \mu^4 \sin\left(\phi_w\right)\cos\left(\gamma\mu^2 \sin\left(\phi_w\right)\right)}{10} \,, \end{aligned} \tag{29}$$

$$A_{42} = -\Omega^2 m_p \,, \tag{30}$$

$$A_{43} = -\frac{\Omega^2 m_p}{10} \,, \tag{31}$$

$$A_{44} = A_{wl} g\rho - M_{vessel}\Omega^2 - \frac{11\Omega^2 m_p}{10} \,, \tag{32}$$

$$A_{45} = A_{wl}CoBg\rho - A_{wl}CoFg\rho - \frac{11\Omega^2 l_0 m_p \sin\left(\gamma\mu^2 \sin\left(\phi_w\right)\right)}{10} - \frac{11g\gamma^2 m_p \mu^6 \sin\left(\gamma\mu^2 \sin\left(\phi_w\right)\right)\cos^2\left(\phi_w\right)}{10} - \frac{11g\gamma m_p \mu^4 \sin\left(\phi_w\right)\cos\left(\gamma\mu^2 \sin\left(\phi_w\right)\right)}{10}, \tag{33}$$

$$A_{51} = -\frac{11\Omega^2 l_0^2 m_p \nu \cos\left(\gamma\mu^2 \sin\left(\phi_w\right)\right)}{10} - \frac{6\Omega^2 l_0^2 m_p \cos\left(\gamma\mu^2 \sin\left(\phi_w\right)\right)}{5}, \tag{34}$$

$$A_{52} = -\Omega^2 l_0 m_p \sin\left(\gamma\mu^2 \sin\left(\phi_w\right)\right), \tag{35}$$

$$A_{53} = -\frac{\Omega^2 l_0 m_p \sin\left(\gamma\mu^2 \sin\left(\phi_w\right)\right)}{10}, \tag{36}$$

$$A_{54} = A_{wl}CoBg\rho - A_{wl}CoFg\rho - \frac{11\Omega^2 l_0 m_p \sin\left(\gamma\mu^2 \sin\left(\phi_w\right)\right)}{10}, \tag{37}$$

$$A_{55} = GM_L Vg\rho - I_5\Omega^2 - \frac{11\Omega^2 l_0^2 m_p \sin^2\left(\gamma\mu^2 \sin\left(\phi_w\right)\right)}{10} - \frac{11\Omega^2 l_0^2 m_p \cos^2\left(\gamma\mu^2 \sin\left(\phi_w\right)\right)}{10} + \frac{11g\gamma l_0 m_p \mu^2 \cos\left(\gamma\mu^2 \sin\left(\phi_w\right)\right)\cos\left(\phi_w\right)}{10} + \frac{11g l_0 m_p \cos\left(\gamma\mu^2 \sin\left(\phi_w\right)\right)}{10}. \tag{38}$$

Calculated formulas (5) and (6) (reduced to the first order) enable a series of numerical simulations of the payload-vessel system to be performed.

4. NUMERICAL SIMULATIONS – COMPARATIVE ANALYSIS

As discussed, the authors conducted numerical analysis in order to give a satisfactory confirmation of the proposed methodology. The considerations concern one-dimensional forward propagating waves as vessel excitation. The following simulations depict a comparative analysis of the payload response results for a number of different payload masses.

The results of simulations for a payload pendulation and vessel heave motion for the subsequent masses up to 10% of a total ship displacement considered in the study are depicted in Figs. 2 and 3 in a form of time domain analysis (payload response) and frequency spectra (vessel heave) for convenience.

The masses examined in the regime of light lifts reveal similar behaviour (Fig. 2) – the higher the subsequent mass, the lower the amplitude of oscillations. The nature of the waveforms remained unchanged and only slight quantitative changes can be observed. This leads to the conclusion of uncoupled analysis for the referenced payload-vessel mass relation. The numerical simulations for the relation above the threshold value 2%, depict a qualitative change clearly observable in the

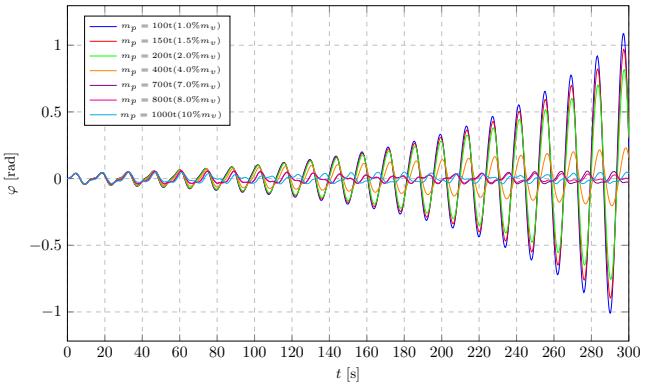

Fig. 2. Payload pendulation – comparative results for different payload weights ($T = 7$ s, $l_0 = 48.7$ m)

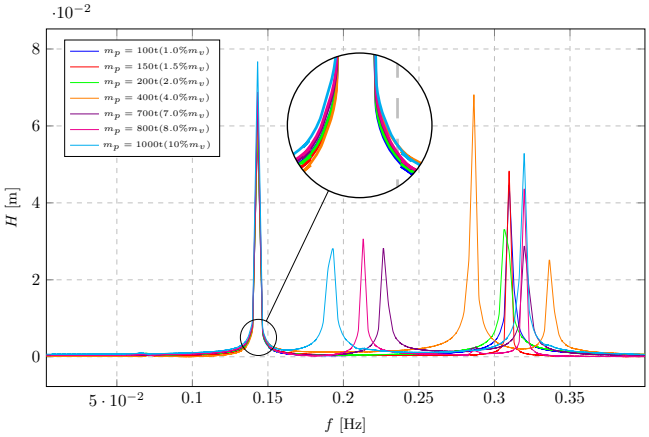

Fig. 3. Vessel heave spectra – comparative results for different payload weights ($T = 7$ s, $l_0 = 48.7$ m)

character of waveforms. The expected divergence in not only quantitative measures is captured immediately past the threshold value while qualitative discrepancy started to appear at around 3–4% of the vessel displacement. The results obtained from the proposed model are consistent with the results of the 3-DoF model proposed in [22] in light lifts regime.

Results for vessel heave (Fig. 3) reveal no significant influence of payload weight on the system frequency structure for the referenced light lifts. Critical harmonic components do not change their position even for the limit value of lifted object mass. The amplitude of dynamic response is marginally lower for the heavier objects (considered still in the light lifts regime) but it does not have a meaningful invalidating impact on the proposed methodology. The authors concept can be useful for resonance recognition in light lifts, even given marginally undervalued amplitudes. However, when considering harmonic components of heavy object lifts, one can notice a clear dependency of the components moving towards lower frequencies and an increase in the value of their amplitudes. This strongly indicates the necessity to analyse coupled systems within heavy lifts regime.

The assumed frequency of the excitation was set equal to $\omega \approx 0.897$ rad s^{-1} ($T = 7$ s), which is for medium-slow waves.

The presented simulation results depict the payload pendulation for the consecutive masses for some specific length of cable ($l_0 \approx 48$ m), causing a parametric resonance to occur in the system. The resonating length is specified based on the excitation frequency. Naturally, the observable parametric resonance will be raised for different cable lengths. However, the examined phenomena and the qualitative results will remain valid. The authors found it valuable to present some additional simulation results prepared for different sets of the system parameters in terms of understanding the proposed methodology.

In order to support the encountered coupling limit between the systems, the authors performed numerical simulations providing a further confirmation for the claimed thesis. The presented results were prepared for a set of different parameters. The frequency of the vessel excitation was set equal to $T = 8$ s and the length of cable was changed to $l_0 \approx 64$ m. Depicted waveforms (Fig. 4) show the same system properties as the results presented in Fig. 2. It can be clearly observed that for the first three consecutive masses (light lift regime), the payload response remains unchanged in terms of quality of the phenomenon while after passing the threshold values, the waveforms expose a visibly different character and amplitude value of payload dynamics.

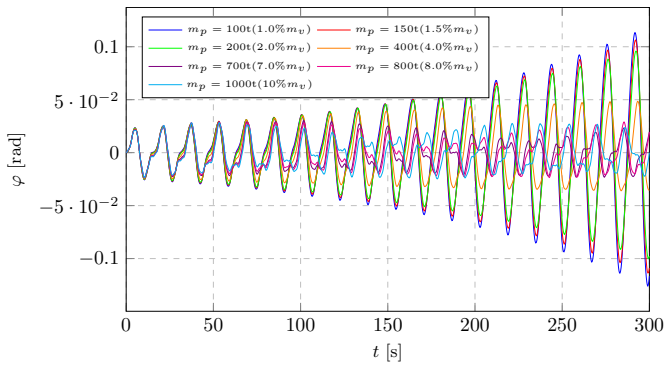

Fig. 4. Payload pendulation – comparative results for different payload weights ($T = 8$ s, $l_0 = 63.6$ m)

A similar trend of the vessel shifting frequencies when lifting heavy objects observed previously in Fig. 3, might also be captured in the spectral analysis of a vessel heave motion presented in Fig. 5. The spectral analysis for the rolling vessel motion reveals the same tendency, however, the level of the amplitudes is of a negligible magnitude and hence it was decided not to be included in the presented results.

The next set of parameters used for the evaluation was prepared and presented for another interesting phenomenon appearing in the system dynamics, being payload oscillation near main resonant vibrations. As can be noticed, regardless of the type of occurring phenomenon, the excitation frequency or the cable length, the established threshold value determining the limit of coupled dynamics considerations, remains unchanged. The simulation results for the excitation period equals $T = 7$ s and length of cable set to $l_0 \approx 12$ m are depicted in Fig. 6. The main resonance vibrations are reached for the payload mass of $m_p = 1\%m_v$ which is to be considered as a lightweight object.

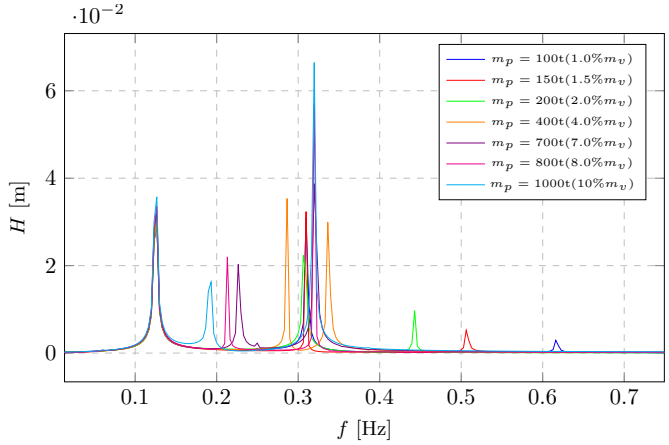

Fig. 5. Vessel heave spectrum – comparative results for different payload weights ($T = 8$ s, $l_0 = 63.6$ m)

The results obtained after passing the threshold value, for the payload mass of $m_p = 3\%m_v$ expose a totally different nature of the payload response reflected in quality and quantity of the pendulation.

A direct comparative analysis presented in Figs. 7 and 9, where the payload responses were compared in pairs of light and heavyweight lifted objects. Figure 7, depicts a comparison

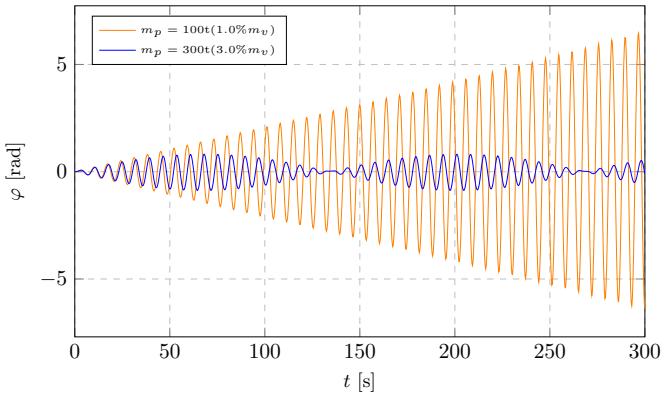

Fig. 6. Payload pendulation – comparative results for different payload weights ($T = 7$ s, $l_0 = 11.7$ m)

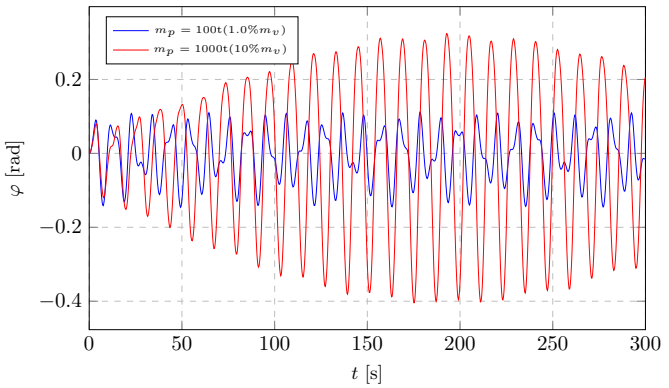

Fig. 7. Payload pendulation – direct comparative results for light and heavy payload weights ($T = 6$ s, $l_0 = 25.9$ m)

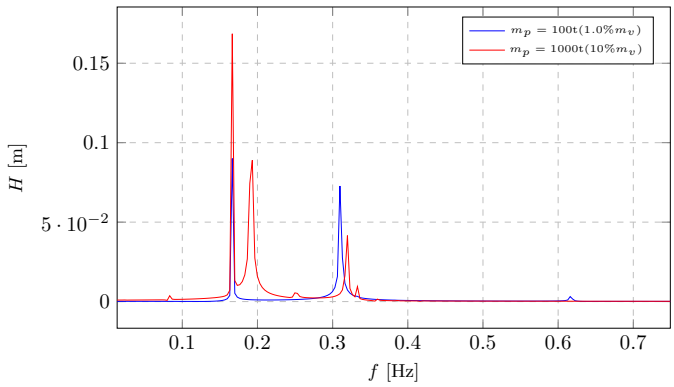

Fig. 8. Vessel heave spectrum – comparative results for different payload weights ($T = 6$ s, $l_0 = 25.9$ m)

between 1% and 10% of the payload mass to vessel displacement ratio. It can be observed that the oscillations differ for each of the mass considered in terms of quality and quantity of the results. The same properties might be seen in Fig. 9, where the floating unit displacement was examined for 1.5% and 9.5%.

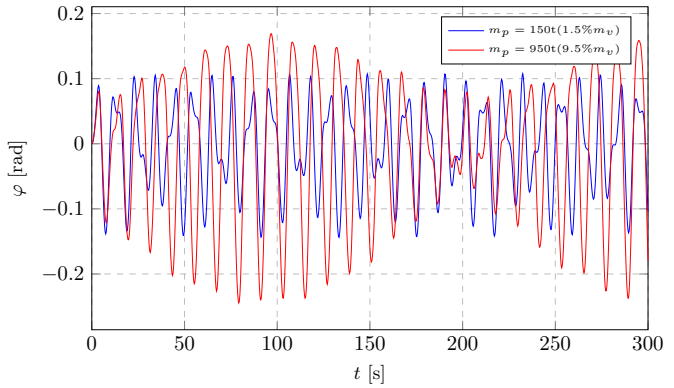

Fig. 9. Payload pendulation – direct comparative results for light and heavy payload weights ($T = 6$ s, $l_0 = 25.9$ m)

Figures 8 and 10 expose the changes that occur for ship dynamics depending on the considered lifting regime. The spectra show the same nature of frequencies shift for heavy lifts towards lower values and their increase in terms of the main component amplitude level as mentioned and observed in Figs. 3, 5, 8 or 10.

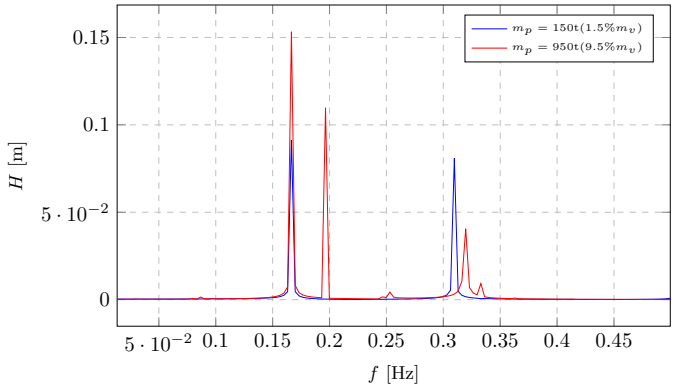

Fig. 10. Vessel heave spectrum – comparative results for different payload weights (= 6 s, $l_0 = 25.9$ m)

5. CONCLUSIONS

Payload mass to ship displacement ratios have been investigated for light and heavyweight lifted objects. The expected discrepancy in quantitative results was observed immediately past the threshold value, while qualitative divergence started to appear at around 3–4%, which confirms the presented model gives satisfactory confirmation of the referenced assumption. The research carried out for similar problems highlights the lack of availability of analytical tools for reliable payload response analysis. One might find sophisticated and complex numerical environments or overly simple dynamic models which are not able to represent the comprehensive payload dynamics beyond the application of the light lifts assumption. The proposed model was used to achieve the best possible efficiency for the problems within light and heavy lifts in the air.

It can be concluded that the demonstrated approach is more widely applicable than analysis of the payload dynamics independently of a vessel. The proposed concept eliminates RAOs as a method of vessel movement representation, as this methodology is only justifiable if the light lifts assumption is fulfilled. For heavy lifts, uncoupled models cannot be utilised as high discrepancies are observed between the presented methodology and models neglecting coupling. Based on the analysis carried out, it can be stated that the model proposed by the authors is more universal and comprehensive, and this is what constitutes its main advantage.

REFERENCES

[1] W.G. Acero, L. Li, Z. Gao, and T. Moan, "Methodology for assessment of the operational limits and operability of marine operations," *Ocean Eng.*, vol. 125, pp. 308–327, 2016, doi: 10.1016/j.oceaneng.2016.08.015.

[2] W. Meng, L.H. Sheng, M. Qing, and B.G. Rong, "Intelligent control algorithm for ship dynamic positioning," *Arch. Control Sci.*, vol. 24, 2014, doi: 10.2478/acsc-2014-0026.

[3] L. Li, Z. Gao, T. Moan, and H. Ormberg, "Analysis of lifting operation of a monopile for an offshore wind turbine considering vessel shielding effects," *Marine Struct.*, vol. 39, pp. 287–314, 2014, doi: 10.1016/j.marstruc.2014.07.009.

[4] H. Zhu, L. Li, and M. Ong, "Study of lifting operation of a tripod foundation for offshore wind turbine," in *IOP Conf. Ser.: Mater. Sci. Eng.*, vol. 276, no. 1, 2017, doi: 10.1088/1757-899X/276/1/012012.

[5] H.-S. Kang, C.H.-H. Tang, L.K. Quen, A. Steven, and X. Yu, "Prediction on parametric resonance of offshore crane cable for lowering subsea structures," in *2016 IEEE International Conference on Underwater System Technology: Theory and Applications (USYS)*. IEEE, 2016, pp. 165–170, doi: 10.1109/USYS.2016.7893905.

[6] H.-S. Kang, C.H.-H. Tang, L.K. Quen, A. Steven, and X. Yu, "Parametric resonance avoidance of offshore crane cable in subsea lowering operation through a* heuristic planner," *Indian J. Geo-Marine Sci.*, 2017.

[7] V. Čorić, I. Ćatipović, and V. Slapničar, "Floating crane response in sea waves," *Brodogradnja: Teorija i praksa brodogradnje i pomorske tehnike*, vol. 65, no. 2, pp. 111–120, 2014.

[8] N. Sun, Y. Wu, H. Chen, and Y. Fang, "An energy-optimal solution for transportation control of cranes with double pendulum dynamics: Design and experiments," *Mech. Syst. Signal Process.*, vol. 102, pp. 87–101, 2018, doi: 10.1016/j.ymssp.2017.09.027.

[9] X. Peng, Z. Geng *et al.*, "Anti-swing control for 2-d underactuated cranes with load hoisting/lowering: A coupling-based approach," *ISA Trans.*, vol. 95, pp. 372–378, 2019, doi: 10.1016/j.isatra.2019.04.033.

[10] Y.-G. Sun, H.-Y. Qiang, J. Xu, and D.-S. Dong, "The nonlinear dyn., and anti-sway tracking control for offshore container crane on a mobile harbor," *J. Marine Sci. Technol.*, vol. 25, no. 6, p. 5, 2017, doi: 10.6119/JMST-017-1226-05.

[11] Q.H. Ngo, N.P. Nguyen, C.N. Nguyen, T.H. Tran, and Q.P. Ha, "Fuzzy sliding mode control of an offshore container crane," *Ocean Eng.*, vol. 140, pp. 125–134, 2017, doi: 10.1016/j.oceaneng.2017.05.019.

[12] X. Xu and M. Wiercigroch, "Approximate analytical solutions for oscillatory and rotational motion of a parametric pendulum," *Nonlinear Dyn.*, vol. 47, no. 1-3, pp. 311–320, 2007, doi: 10.1007/s11071-006-9074-4.

[13] D. Yurchenko and P. Alevras, "Stability, control and reliability of a ship crane payload motion," *Probab. Eng. Mech.*, vol. 38, pp. 173–179, 2014, doi: 10.1016/j.probengmech.2014.10.003.

[14] X. Zhao and J. Huang, "Distributed-mass payload dynamics and control of dual cranes undergoing planar motions," *Mech. Syst. Signal Process.*, vol. 126, pp. 636–648, 2019, doi: 10.1016/j.ymssp.2019.02.032.

[15] Z. Ren, A.S. Verma, B. Ataei, K.H. Halse, and H.P. Hildre, "Model-free anti-swing control of complex-shaped payload with offshore floating cranes and a large number of lift wires," *Ocean Eng.*, vol. 228, 2021, doi: 10.1016/j.oceaneng.2021.108868.

[16] N.-K. Ku, J.-H. Cha, M.-I. Roh, and K.-Y. Lee, "A tagline proportional–derivative control method for the anti-swing motion of a heavy load suspended by a floating crane in waves," *Proc. Inst. Mech. Eng., Part M: J. Eng. Marit. Environ.*, vol. 227, no. 4, pp. 357–366, 2013, doi: 10.1177/1475090212445546.

[17] S. Robak and R. Raczkowski, "Substations for offshore wind farms: A review from the perspective of the needs of the polish wind energy sector," *Bull. Pol. Acad. Sci. Tech. Sci.*, vol. 66, no. 4, 2018, doi: 10.24425/124268.

[18] "Recommended practice modelling and analysis of marine operations n103," *DET NORSKE VERITAS GL*, pp. Sec. 9.2–9.3, 2017.

[19] "Recommended practice c205 environmental conditions and environmental loads," *DET NORSKE VERITAS GL*, p. Sec. 3.3.2, 2010.

[20] *Fathom Group Ltd. Engineering Procedure*, 2018.

[21] P. Boccotti, *Wave mechanics and wave loads on marine structures*. Butterworth-Heinemann, 2014.

[22] B. Chilinski, A. Mackojc, R. Zalewski, and K. Mackojc, "Proposal of the 3-dof model as an approach to modelling offshore lifting dynamics," *Ocean Eng.*, vol. 203, pp. 287–314, 2020, doi: 10.1016/j.oceaneng.2020.107235.